J. Mater. Shaping Technol. (1991) 9:153–159

The Determination of Optimum Blank Shapes When Deep Drawing Prismatic Cups

F. Liu and R. Sowerby

Abstract. The article discusses some techniques for the determination of ideal (or optimum) blank contours when deep drawing prismatic cups. The ideal contours are designed to produce essentially flat topped cups and thus trimming of excess material is minimized. The techniques lend themselves to such processes where the cups are drawn from initially flat blanks in the presence of a blank holder. Tooling which involves lock beads or draw beads is not considered.

Attention is devoted to two techniques developed by the authors; each method is based on the solution of Laplace's equation. One technique is experimental and uses an electrostatic analogue, the second is numerical and the solution procedure employs the boundary element method. Neither method attempts a rigorous analysis of the actual drawing operation. They are intended as a means of producing near-net shaped blanks with little computational effort. Since material costs usually represent a major portion of the overall cost of a sheet metal part, the theme of the paper has immediate practical significance.

Introduction

Material costs are usually a major portion of the overall cost of a sheet metal component. One way of reducing scrap is to minimize the amount of material trimmed from the part. For deep drawn prismatic cups, when constraints to material flow are due only to a blank holder or hold down plate, it is possible to predict near-net shape (or optimum) blanks, which will result in savings of material. Several techniques are available and some of the more popular methods are reviewed here.

Nowadays, finite element analysis is the favored numerical method for modelling sheet metal deformation processes. The formulation can be very sophisticated, and finite element codes can be obtained which can accommodate large strain and large displacement (rotation) processes, anisotropy, elastic–plastic material behavior, membrane and bending elements, and different plasticity theories, such as incremental, deformation, and vertex theories.

Considerable attention has been paid to modelling axisymmetric deformation processes like punch stretching and deep drawing, and with some effort theoretical results can be obtained which agree quite well with experimental observations [1]. The application of the same methods to the deep drawing of other than axisymmetric shapes has been less successful. In these studies, the initial blank shape is specified, and very few papers have appeared in the open literature which deal with the development of near-net shaped blanks using a finite element method.

One example is the work of Toh and Kobayashi [2] who predicted optimum blank shapes when deep drawing square cups. The main thrust of the article was the analysis of the drawing process starting with either a circular, square, or octagonal blank. A knowledge of the flow patterns for each of the different blank shapes would certainly give some indication of the form of the optimum shape. The algorithm for producing the optimum shape was not

The authors are with the Department of Mechanical Engineering, McMaster University, Hamilton, Ontario, Canada.

discussed in detail in the article. However, experimental data were provided of square cups drawn from the predicted ideal blank contours, and the results were quite good.

In Ref. [3], the deep drawing of square and elliptical cups was studied both experimentally and theoretically. The initial blank contour was circular and no attempt was made to develop optimum profiles. However, predicted flow patterns were provided along with the contour of the deforming blank at different stages in the drawing process; these predictions compared very well with the experimental results. A knowledge of the flow patterns for circular blanks will also provide some indication of the optimum blank shapes. The finite element programs developed in Refs. [2] and [3] were designed to analyze the entire deep drawing process. If the goal is an estimate only of the ideal blank contour, then simpler codes could be developed.

Slip line field (SLF) theory [4] has been applied to analyze the deformation in the flange when drawing irregular shaped cups [5]. At first sight SLF analysis would appear to be of limited practical worth, since the theory (in its simplest form) deals with a nonhardening solid and assumes no change in the thickness of the flange. Furthermore, since the boundary of the blank is changing during the drawing process, it might be anticipated that this would present problems in developing appropriate SLF patterns.

However, the utility of the SLF method for developing optimum shaped blanks was demonstrated by Lange and his coworkers [6,7]. It was assumed that the die contour and the perimeter of the blank are principal stress directions, and hence the slip lines intersect these boundaries at ± 45 deg. If the die contour can be made up of straight lines and circular arcs (which in general would always be true), then it is easy to extend the SLF into the flange. Under these circumstances the starting slip lines, that is, those emanating from the die contour, are always straight lines and logarithmic spirals, and providing the die contour is everywhere convex outwards the field can be extended either graphically or numerically with equal facility. It was pointed out in Ref. [7] that many of the slip line fields developed in this manner failed to satisfy the Hencky equations, which means that the fields are in error. Nevertheless, the fields can still be used to develop blank contours. It can be demonstrated [7,8] that for each blank profile constructed, the time taken for particles to flow from the blank boundary to the die contour along the individual stream lines is always the same. Each particle on the blank boundary reaches the die contour at the same time, thus producing a flat topped cup. In this sense the blank contours are ideal.

In Ref. [8] computer programs were developed to run on a microcomputer. The programs calculate the SLF mesh (and associated hodograph), the blank contour, and stream lines for any convex outward punch profile. The flow is ideal since the blank contours and the stream lines form an orthogonal network of lines. The calculation time to produce several successive blank contours (corresponding to different draw depths) is 2 to 3 minutes. A hard copy of the blank contours can be obtained from a plotter or laser printer. The authors have performed a number of experiments (see Ref. [8]) on the deep drawing of square cups, using square punches of different geometry. Optimum blanks were developed using SLF theory. The resulting cups were not flat topped, but the undulations around the rim were quite small.

Note that when the punch contour possesses reentrant regions, such as L shaped punches, the extension of the slip line field into the flange is limited. At some stage in the development of the field one family of slip lines run together and the field cannot be continued.

In the following section two techniques, developed by the authors, for producing optimum blank shapes are described. Each technique is based on the solution of Laplace's equation. One method is experimental and the other numerical; in either case no restriction is placed on the shape of the punch contour.

Methods of Evaluating Optimum Blanks

Electrostatic Analogue Method

Since Laplace's and Poisson's equations arise in many areas of applied physics and engineering, extensive efforts have been made to finding methods for their solution. The use of analogue techniques as a method of solution is well documented [9,10]. In this section an electrical analogue for blank development is described. This is not the first time an electrical analogue has been used to determine blank shapes. Zhaotao and Bingwen [11] used an electrolytic tank, built according to a specification by Boothroyd et al. [12]. In the present work a conductive sheet analogue [10] is employed, and this is considered to be cheaper and easier to use than the electrolytic tank method.

The equilibrium equations for the plane strain,

quasistatic deformation of an incompressible solid are

$$\frac{\partial \sigma_{xx}}{\partial x} + \frac{\partial \sigma_{xy}}{\partial y} = 0$$
$$\frac{\partial \sigma_{yy}}{\partial y} + \frac{\partial \sigma_{yx}}{\partial x} = 0 \quad (1)$$

while the continuity equation is

$$\frac{\partial v_x}{\partial x} + \frac{\partial v_y}{\partial y} = 0 \quad (2)$$

If the material obeys the von Mises yield criterion and Levy-Mises flow rule, then as demonstrated in Ref. [11], the hydrostatic pressure obeys Laplace's equation. This was the basis for the analogy drawn by Zhaotao and Bingwen [11]. We want to make the analogy by assuming the flow of the material in the flange of the drawn cup is comparable to the irrotational flow of an inviscid liquid. It was mentioned in the previous section that an outcome of the SLF solution was that the contours of the blank profiles and the stream lines form an orthogonal network of lines. This is a characteristic of the flow of an ideal liquid where the flow lines are orthogonal to contours of equipotential, Φ, and the velocity components are derivable from Φ. It is easy to prove that the velocity potential obeys Laplace's equation:

$$\frac{\partial^2 \Phi}{\partial x^2} + \frac{\partial^2 \Phi}{\partial y^2} = 0 \quad (3)$$

The voltage (E) distribution in an isotropic, conductive sheet of uniform thickness can also be shown to obey Laplace's equation

$$\frac{\partial^2 E}{\partial x^2} + \frac{\partial^2 E}{\partial y^2} = 0 \quad (4)$$

For a more detailed discussion on the analogy between Eqs. (3) and (4), see Ref. [13]. The conductive sheet analogue allows the determination of contours of equal E, which correspond to contours of equal velocity potential, Φ, and hence the ideal blank contours.

The experimental technique is shown schematically in Figure 1. The conductive sheet is sold commercially in a variety of cut sizes or in roll form; the sheet thickness is about 0.15 mm. Ideally the paper should be uniform in thickness, with a smooth surface finish, and possess a high, but uniform, resistivity. The profile of the punch is drawn on one surface using conductive ink or paint. We applied conductive ink using a standard drafting pen. An outer boundary is then drawn (convex outwards) on the paper, as far away as possible from the punch boundary. A 10 V dc battery was connected across the two boundaries as shown in Figure 1. A steel pointed stylus attached to a high impedance voltmeter (in order that negligible current is drawn from the circuit) is used to map out contours of equipotential, which represent the ideal blank contours. A

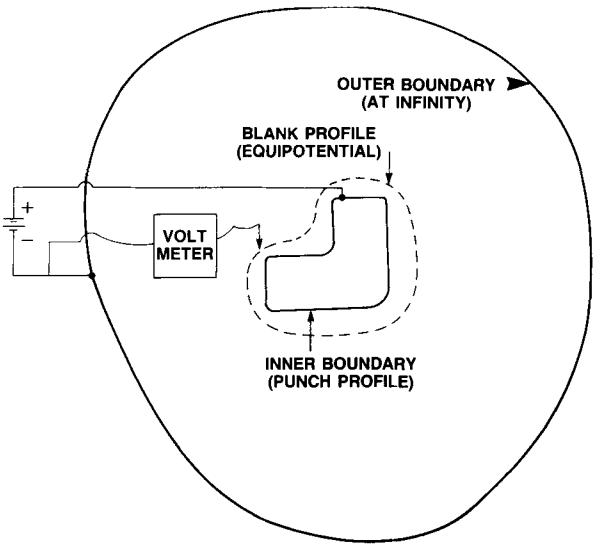

Fig. 1. Circuit diagram for the electrical (conductive sheet) analogue.

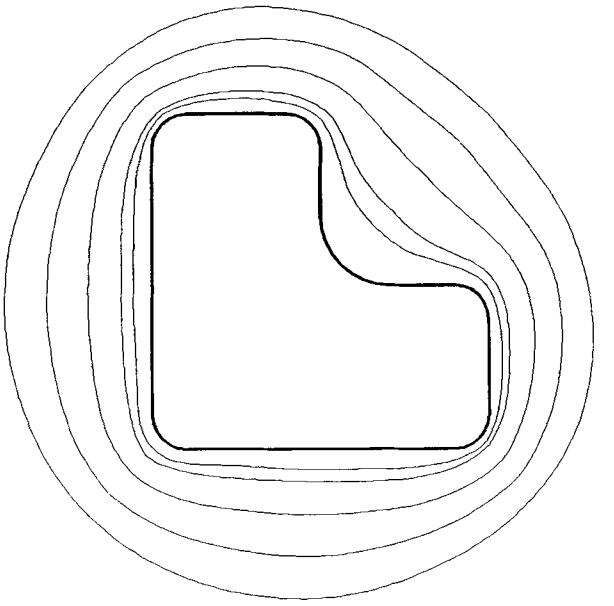

Fig. 2. Blank contours for an L shaped cup using the conductive sheet analogue.

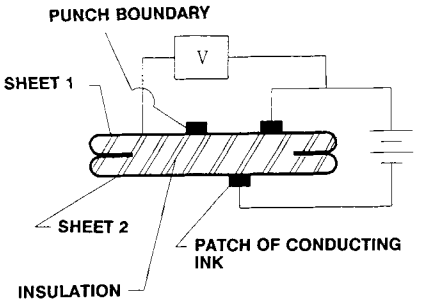

Fig. 3. Alternative circuit diagram to Fig. 1.

succession of nested contours correspond to blank profiles for different draw depths. Profiles generated for the deep drawing of L shaped cups are shown in Figure 2.

Large sheets of resistance paper are required if the outer boundary is to be drawn far away from the punch profile boundary. As an alternative, the arrangement shown in Figure 3 can be adopted. Two circular pieces of resistance paper are used, they are joined around the periphery, but insulated from each other everywhere else. On the surface of one sheet the punch profile is drawn using conductive ink, while a small patch of conductive ink is deposited at the center of the second sheet. It can be demonstrated [12] that this small patch of ink is equivalent to a pole (or boundary) at infinity. Both experimental arrangements were employed, and yielded essentially the same results for the equipotential contours.

Boundary Element Method

The various ways of solving Laplace's equation were mentioned above and the analogy was drawn between the irrotational flow of an inviscid liquid and the ideal flow of the material in the flange of a drawn cup. The same analogy is used here, but Eq. (3), involving the velocity potential Φ, is solved using a numerical technique referred to as the boundary element method [14,15].

Figure 4 is a schematic representation of the punch boundary, Γ_1, the current boundary, Γ_2, of the ideal blank, and the domain, Ω, which represents the flange. It is assumed that Φ is a constant along the boundary Γ_2, and that the inward velocity (say, q) is normal to Γ_2. How the boundary Γ_2 is determined will be indicated later. It is further assumed that on the punch boundary Γ_1 the flow is normal to the boundary and is a constant along the boundary. Hence Φ is unknown along Γ_1 and q is unknown along Γ_2. However, $q = \partial\Phi/\partial n$ where n is the inward normal to the

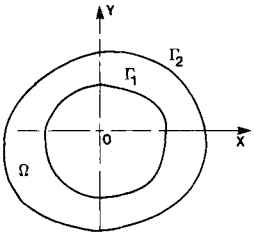

Fig. 4. Schematic representation of the inner (punch) and outer (blank) boundaries in the boundary element method.

boundary. With these conditions there exists a well-posed problem of the Laplace type with

$$\begin{aligned} \nabla^2\Phi &= 0 && \text{in } \Omega \\ \Phi &= \bar{\Phi} \text{ (say)} && \text{on } \Gamma_2 \\ q &= \bar{q} \text{ (say)} && \text{on } \Gamma_1 \end{aligned} \tag{5}$$

The above set of equations can be solved by the method of "weighted residuals," which are taken to be Green's function belonging to the Laplacian operator in two dimension. The theoretical fundamentals are covered in Refs. [14–16], where it is demonstrated that the above equations can be restated in the form of a boundary integral equation

$$c_i\Phi_i + \int_\Gamma \Phi q^* d\Gamma = \int_\Gamma q\Phi^* d\Gamma \tag{6}$$

where $\Gamma = \Gamma_1 + \Gamma_2$, i is a generic source point (in this work only points on the boundary are considered), and Φ_i is the corresponding potential; c_i is a coefficient and can be determined if the shape of the boundary is known at i. The quantity Φ^* is the weighted residual defined as

$$\Phi^* = \frac{1}{2\pi} \ln\left[\frac{1}{r}\right] \tag{7a}$$

and

$$q^* = \frac{\partial\Phi^*}{\partial\bar{n}} \tag{7b}$$

In Eq. (7a) r is a position vector from a source point on the boundary to any other boundary point.

When solving the integral Eq. (6), by the boundary element method, the approach is to discretize the equation into a system of elements on the boundary. Linear elements were employed in the present work, and hence Φ and q vary linearly over each element and can be expressed in terms of the nodal point values. Ultimately the equations will be integrated numerically using a four-point Gaussian quadrature,

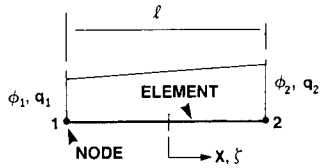

Fig. 5. Linear elements and a local dimensionless coordinate system.

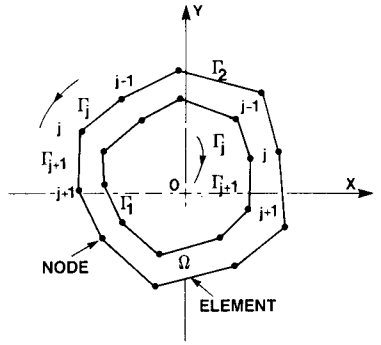

Fig. 6. Discretization of boundaries.

and it is convenient to introduce a dimensionless local coordinate, ξ, to define the linear elements, see Figure 5. The values of Φ and q can now be expressed as

$$\Phi(\xi) = S_1\Phi_1 + S_2\Phi_2$$
$$q(\xi) = S_1q_1 + S_2q_2 \tag{8}$$

where the dimensionless coordinate ξ equals $x/(\ell/2)$ and

$$S_1 = (1 - \xi)/2 \quad \text{and} \quad S_2 = (1 + \xi)/2$$

To keep the normal of the boundary outwards over the domain Ω, the inner boundary Γ_1 is discretized in a clockwise manner and the outer boundary Γ_2 anticlockwise, as illustrated in Figure 6. Each boundary contains N elements. Equation (6) in discretized form can be written

$$c_i\Phi_i + \sum_{j=1}^{2N} \int_{\Gamma_j} \Phi q^* d\Gamma = \sum_{j=1}^{2N} \int_{\Gamma_j} q\Phi^* d\Gamma \tag{9}$$

The method of integrating over the j segment can be demonstrated by considering the integral term on the left hand side of Eq. (9); by using Eq. (8) it can be written as

$$\int_{\Gamma_j} \Phi q^* d\Gamma = [h_{ij}^1 h_{ij}^2] \begin{Bmatrix} \Phi_1 \\ \Phi_2 \end{Bmatrix} \tag{10}$$

where

$$h_{ij}^1 = \int_{\Gamma_j} S_1 q^* d\Gamma \quad \text{and} \quad h_{ij}^2 = \int_{\Gamma_j} S_2 q^* d\Gamma$$

and q^* is defined in Eq. (7b).

The method is similar for integrating over the j segment on the right hand side of Eq. (9). Note these integrals can now be evaluated numerically using Gaussian quadrature. Details can be found in Refs. [14,16] along with a discussion on how the discretized terms can be assembled. In the book by Brebbia [14], detailed Fortran computer programs are provided for solving the discretized integral equation. As demonstrated in Refs. [14,16], when all the nodes are considered and the various terms assembled, there results a $2N \times 2N$ system of equations which can be expressed in matrix form

$$[H][\Phi] = [G][q] \tag{11}$$

where each term in $[H]$, defined as H_{ij}, represents the sum of the h^2 term of element $(j - 1)$ and the h^1 term of element j, and similarly for the $[G]$ matrix. The matrices can be partitioned in the following manner

$$\begin{vmatrix} H_{1/1} & H_{1/2} \\ \\ H_{2/1} & H_{2/2} \end{vmatrix} \begin{Vmatrix} \Phi_1 \\ \vdots \\ \Phi_N \\ \vdots \\ \Phi_{N+1} \\ \vdots \\ \Phi_{2N} \end{Vmatrix} = \begin{vmatrix} G_{1/1} & G_{1/2} \\ \\ G_{2/1} & G_{2/2} \end{vmatrix} \begin{Vmatrix} q_1 \\ \vdots \\ q_N \\ \vdots \\ q_{N+1} \\ \vdots \\ q_{2N} \end{Vmatrix} \tag{12}$$

The notation $H_{1/1}$ implies nodes on the inner boundary with integration being carried out over elements on the inner boundary; while $H_{2/1}$ implies nodes on the outer boundary with the integration over elements on the inner boundary, etc. It is a simple matter to rearrange Eq. (12) to solve for the unknowns $\Phi_1 \rightarrow \Phi_N$, and $q_{N+1} \rightarrow q_{2N}$.

In the present case we analyzed the drawing problem by successively moving back the outer boundary. The solution was started from the inside boundary (the punch profile boundary) Γ_1. The velocity q at each node on the inner boundary is assumed constant and therefore by selecting a time step Δt, each node was stepped back a distance $q\Delta t$. This established the first outer boundary Γ_2. The node is moved back in a normal direction, and an averaging technique was developed using the normal direction of each adjacent element. With boundary Γ_2 in position, the elements of the matrices in Eq. (11) were evaluated along with the unknown q values over the outer

boundary. Once having solved for the q values, the time step can be repeated using an average value of the nodal velocities at the inner and outer boundary. This refinement is not really necessary if the time step Δt is small enough. With the known values of q on the outer boundary, a new outer boundary is formed in the manner just indicated. The elements of the H and G matrices are now formed between the inner boundary Γ_1 (this never changes) and the new outer boundary. Each successive outer boundary corresponds to an ideal blank contour.

An important property of the H matrix in Eqs. (11) and (12) is that the sum of the elements in any row is zero. A full discussion on this point is provided in Ref. [14]. This particular property of the H matrix makes it possible to choose any constant value, Φ, for the nodal potential, Φ_{N+1} to Φ_{2N}, on the outer boundary Γ_2. It follows that any constant value of Φ on Γ_2 has no influence on the computed nodal velocities, q_{N+1} to q_{2N}, or Γ_2. Only the values of Φ on the inner boundary Γ_1 are affected, and these do not influence the construction of the boundary Γ_2. In our work we selected $\Phi = 0$, for simplicity.

Calculations were performed for a variety of punch shapes. Some predicted profiles for a L shaped punch and square punch are shown in Figures 7 and 8. For the plane strain deformation of an incompressible material the following relationship must hold

$$\oint_{\Gamma_1} q d\Gamma = \oint_{\Gamma_2} q d\Gamma = \text{constant} \qquad (13)$$

The condition was checked for several of the newly created outer boundaries and was found to hold.

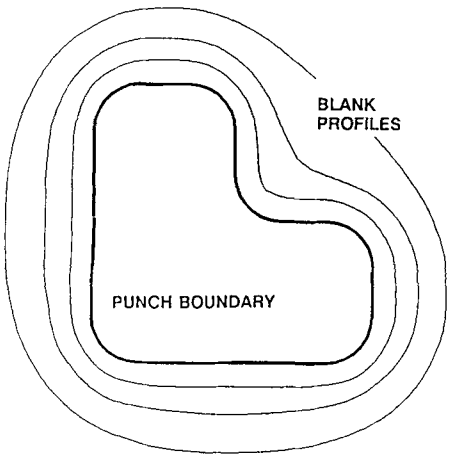

Fig. 7. Predicted optimum blank for an L shaped cup using the boundary element method.

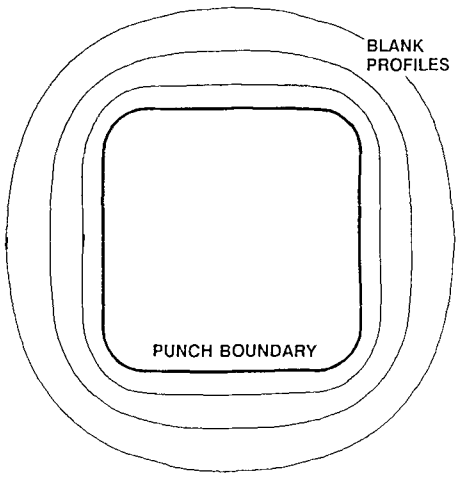

Fig. 8. Predicted optimum blank shapes for a square cup using the boundary element method.

Conclusions

Industrial stamping operations are difficult to model, and blank development is but one aspect of a complicated process. The techniques of blank development described in the article are not exact, since they do not attempt to model the forming process. Furthermore, they apply only to the situation where an initially flat blank is drawn into a prismatic cup in the presence of a blank holder; additional constraints through draw beads, etc., are not considered. In spite of these limitations, we consider each technique can result in material savings with little experimental or computational effort.

Finite element codes which are designed to model the entire forming process are more difficult to formulate than the boundary element method. There are numerous finite element packages which are commercially available, but they tend to be costly. A finite element approach does not necessarily result in an improved optimum blank shape, primarily because the contact conditions between the tooling and the workpiece are not known precisely.

Acknowledgments. The authors would like to thank the Natural Sciences and Engineering Research Council of Canada and the Manufacturing Research Company of Ontario for financial support of this work.

References

1. R.D. Wood, K. Mattiasson, M.E. Honner, and O.C. Zienkowicz (1986). Viscous Flow and Solid Mechanics Approaches to the Analysis of Thin Sheet Forming,

in *Computer Modeling of Sheet Metal Forming Processes* (Eds. N-M. Wang and S.C. Tang), pp. 121–130, The Metallurgical Society, Warrendale, Pennsylvania.
2. C.H. Toh and S. Kobayashi (1985). Deformation Analysis and Blank Design in Square Cup Drawing, *Int. J. Machine Tool Design and Res.*, Vol. 25, pp. 15–32.
3. H. Iseki and T. Murota (1984). Analysis of Deep Drawing of Non-Axisymmetric Cups by the Finite Element Method, Proc. 1st ICTP, pp. 678–684, Tokyo.
4. W. Johnson, R. Sowerby, and R.D. Venter (1982). *Plane Strain Slip Line Fields for Metal Deformation Processes*, Pergamon Press, Oxford, U.K.
5. T. Jimma (1970). Deep Drawing of Convex Polygon-Shells, *J. Japan Soc. Technology for Plasticity*, Vol. 11, pp. 653–660 (in Japanese).
6. V.V. Hazek and K. Lange (1979). Use of the Slip Line Field Method in Deep Drawing Large Irregular Shaped Components, Proc. 7th NAMRC, pp. 65–71, SME.
7. H. Gloeckl and K. Lange (1983). Computer Aided Design of Blanks for Deep Drawn Irregular Shaped Components, Proc. 11th NAMRC, pp. 243–251, SME.
8. R. Sowerby, N. Chandrasekaren, X. Chen, M. Rooks, and P. Correa (1988), The Development of Computer Aids for Sheet Metal Stampings, in *CAD/CAM and FEM in Metalworking*, S.K. Ghosh and A. Niku-Lari, eds., pp. 187–203, Pergamon Press.
9. W. Karplus (1958). *Analog Simulation*, McGraw-Hill Co., New York.
10. W. Karplus and W.W. Soroka (1959). *Analog Methods*, McGraw-Hill Co., New York.
11. Z. Zhaotao and L. Bingwen (1986). Determination of Blank Shapes for Drawing Irregular Cups Using an Electrical Analogue Method, *Int. J. Mech. Sci.*, Vol. 28, pp. 499–503.
12. A.R. Boothroyd, E.C. Cherry, and R. Maker (1949). An Electrolytic Tank for the Measurement of Steady-State Response, Transient Response and Allied Properties of Networks, Proc. IEEE, Vol. 96, pp. 163–170.
13. E. Weber (1950). *Electromagnetic Fields: Vol. 1, Mapping of Fields*, John Wiley and Sons, New York.
14. C.A. Brebbia (1978). *The Boundary Element Method for Engineers*, Halsted Press, New York.
15. C.A. Brebbia, J.C.F. Telles, and L.C. Wrobel (1984). *Boundary Element Techniques*, Springer-Verlag, Berlin.
16. G.S. Gipson (1987). *Boundary Element Fundamentals*, Computational Mechanics Publications, Southampton, U.K.